
GRACE: Gradient-aligned Reasoning Data Curation for Efficient Post-training

Junjie Li*

Harbin Institute of Technology, Shenzhen, China
22b351018@stu.hit.edu.cn

Ziao Wang*

Hong Kong Baptist University, China
ziaowang@hkbu.edu.cn

NingXuan Ma

Harbin Institute of Technology, Shenzhen, China
2023311G27@stu.hit.edu.cn

Jianghong Ma[†]

Harbin Institute of Technology, Shenzhen, China
City University of Hong Kong, China
majianghong@hit.edu.cn

Xiaofeng Zhang[†]

Harbin Institute of Technology, Shenzhen, China
zhangxiaofeng@hit.edu.cn

Abstract

Existing reasoning data curation pipelines score whole samples, treating every intermediate step as equally valuable. In reality, steps within a trace contribute very unevenly, and selecting reasoning data well requires assessing them individually. We present GRACE, a gradient-aligned curation method that views each reasoning trace as a sequence of optimization events and scores every step by two complementary signals: its alignment with the answer-oriented gradient direction, and its consistency with the preceding reasoning trajectory. Step-level scores are aggregated into a sample-level value for subset selection, using only the model’s internal optimization signals and no external reward models or step annotations. To make this scalable, GRACE introduces a representation-level gradient proxy that estimates step-level alignment from token-level upstream signals in a single forward pass. Post-training Qwen3-VL-2B-Instruct on MMathCoT-1M, GRACE reaches 108.8% of the full-data performance with 20% of the data and retains 100.2% with only 5%, with subsets that transfer effectively across model backbones.

1 Introduction

Large-scale reasoning datasets have become a cornerstone for post-training large language and vision-language models [1, 2]. The standard way to use them is to supervise the model on the entire reasoning trace, treating every step as an equally valuable target. In reality, the steps within a trace contribute very unevenly: some directly support the final answer, while others restate earlier content, explore irrelevant tangents, or introduce noise. Training on them uniformly wastes budget on low-value steps and dilutes the contribution of useful ones. This cost has become significant as reasoning corpora grow to millions of traces [3] and post-training takes hundreds of GPU-hours per run. Choosing what to train on therefore matters [4], and for reasoning data this means assessing steps individually rather than ranking whole traces.

*These authors contributed equally to this work.

[†]Corresponding author.

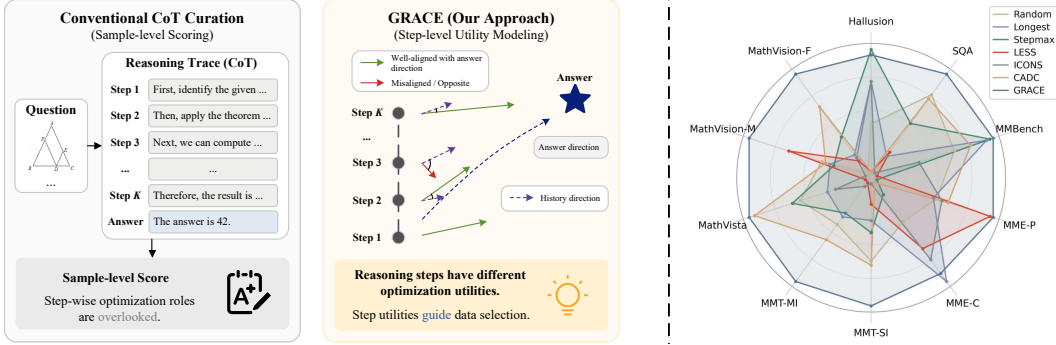


Figure 1: Motivation and empirical effect of GRACE. Left: Reasoning traces are viewed as sequences of optimization events, where each step induces an update direction whose utility depends on its alignment with the target objective and the evolving trajectory. Right: Radar chart comparing downstream performance across benchmarks. GRACE achieves full-data or better performance using only a fraction of the training data.

Existing data curation methods improve training efficiency by selecting samples based on correctness [5], reward models [6], or sample-level influence [7–9] and all of them operate at the granularity of entire traces. As a result, a trace with correct final answers but poor intermediate steps [10] is treated as equally valuable as a tightly reasoned one. This highlights a fundamental limitation: *current approaches lack a mechanism to assess how individual reasoning steps contribute to optimization*.

In this work, we revisit reasoning data from an optimization perspective. Instead of viewing reasoning traces as static supervision targets, we model them as sequences of optimization events, where each reasoning step induces a local training signal that affects the gradient direction toward the final answer. From this view, the utility of reasoning data depends not only on external attributes such as correctness or length, but also on whether its intermediate steps constructively support optimization.

Building on this view, we propose **GRACE** (**G**radient-aligned **R**easoning **d**Ata **C**uration for **E**fficient post-training), a method that performs fine-grained data curation by estimating step-level optimization utility. Rather than pruning or rewriting reasoning traces, GRACE assigns each step a utility score based on two complementary criteria: (i) its alignment with the answer-oriented optimization direction, and (ii) its consistency with the accumulated reasoning trajectory. These signals capture both task-driven and trajectory-aware contributions of each step. The resulting step-level scores are then aggregated to produce a sample-level utility score, enabling effective subset selection while preserving the simplicity of sample-level training. Fig. 1 illustrates the motivation of GRACE and provides empirical evidence that optimization-aware curation can retain strong performance with substantially fewer training samples.

A key challenge is that true step-level gradients are computationally intractable at scale. Naively computing gradients for each reasoning step would require decomposing traces into multiple training instances and performing repeated backward passes. To address this, GRACE introduces a **representation-level gradient proxy** that approximates step-induced optimization directions using token-level upstream signals. This proxy enables efficient estimation of step-level alignment from a single forward pass, making optimization-aware curation practical for large-scale CoT datasets.

We evaluate GRACE by post-training Qwen3-VL-2B-Instruct [11] on MMathCoT-1M [3] and assessing the resulting models on a diverse suite of multimodal benchmarks spanning mathematical reasoning and general visual question answering. GRACE consistently identifies high-value subsets: training on only **20%** of the curated data surpasses full-data performance, reaching **108.8%** of the full-data result averaged across benchmarks, while using only **5%** retains **100.2%**. Furthermore, the selected subsets transfer effectively across model backbones, suggesting that the proposed optimization-based signal captures intrinsic data value beyond a specific model configuration.

Our contributions are three-fold:

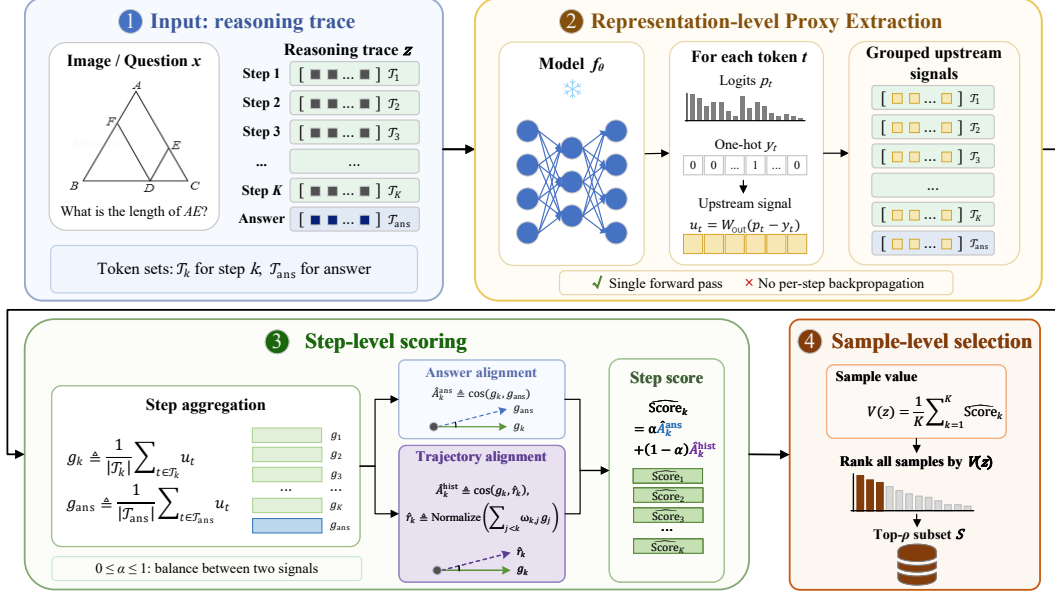


Figure 2: The GRACE curation pipeline. (1) Given an input and its reasoning trace, GRACE identifies token sets for each step and the answer. (2) A fixed scoring model extracts token-level upstream signals in one forward pass and groups them by token sets. (3) Grouped signals are averaged into gradient proxies and scored by answer and trajectory alignment. (4) Step scores are aggregated into a sample value for ranking and top- ρ subset selection.

1. We introduce an optimization-based perspective on reasoning data, framing reasoning traces as sequences of optimization events and highlighting the role of step-level alignment in effective learning.
2. We propose GRACE, a reasoning data curation method that aggregates step-level optimization signals derived from answer-oriented alignment and trajectory consistency for sample-level subset selection.
3. We develop a representation-level gradient proxy that enables scalable estimation of step-level alignment without per-step parameter-space gradient computation.

2 Method

In this section, we present GRACE. We first define the reasoning data curation problem, then derive the step-level optimization utility, introduce its scalable representation-level proxy, and describe sample-level subset selection. The overall pipeline is illustrated in Fig. 2.

2.1 Problem Formulation

We consider a reasoning dataset $\mathcal{D} = \{z_i\}_{i=1}^N$, where each sample is

$$z_i = (x_i, \mathbf{s}_i, a_i),$$

with x_i denoting the input, $\mathbf{s}_i = (s_{i,1}, s_{i,2}, \dots, s_{i,K_i})$ denoting a sequence of reasoning steps, and a_i denoting the final answer. Let f_θ denote the model, and let $\mathcal{T}_{i,k}$ and $\mathcal{T}_{i,ans}$ denote the token positions of step $s_{i,k}$ and the answer segment, respectively. For any token set \mathcal{T} , we define the average token-level loss

$$L(\theta; z_i, \mathcal{T}) = \frac{1}{|\mathcal{T}|} \sum_{t \in \mathcal{T}} L_t(\theta; z_i).$$

Accordingly, the step loss and answer loss are given by $L_{i,k} = L(\theta; z_i, \mathcal{T}_{i,k})$ and $L_i^{\text{ans}} = L(\theta; z_i, \mathcal{T}_{i,\text{ans}})$, and the full loss over the reasoning trace and answer is

$$\mathcal{T}_{i,\text{full}} = \bigcup_{k=1}^{K_i} \mathcal{T}_{i,k} \cup \mathcal{T}_{i,\text{ans}}, \quad L_{\text{full}}(\theta; z_i) = L(\theta; z_i, \mathcal{T}_{i,\text{full}}).$$

Standard post-training minimizes

$$\mathcal{L}_{\text{SFT}}(\theta; \mathcal{D}) = \frac{1}{|\mathcal{D}|} \sum_{z_i \in \mathcal{D}} L_{\text{full}}(\theta; z_i). \quad (1)$$

Our goal is to select a compact subset $\mathcal{S} \subset \mathcal{D}$ with budget $|\mathcal{S}| = \lceil \rho |\mathcal{D}| \rceil$, where $\rho \in (0, 1)$ is the selection ratio, such that post-training on \mathcal{S} preserves or improves downstream performance compared with training on the full dataset. To this end, GRACE assigns each sample a scalar value score $V(z_i)$ and selects the top-ranked subset:

$$\mathcal{S} = \{z_i \in \mathcal{D} \mid \text{rank}_V(z_i) \leq \lceil \rho |\mathcal{D}| \rceil\}. \quad (2)$$

The key question is how to define $V(z_i)$ for reasoning data. GRACE addresses this by estimating the optimization utility of each reasoning step and aggregating these step-level signals into a sample-level value. Since these values are computed from model-internal signals, the scoring model should provide stable representations. Following prior works [12, 13], we obtain the scoring model f_θ by warming up an initial model f_{θ_0} on a γ -ratio subset of \mathcal{D} , and keep it fixed during data scoring.

2.2 Step-level Optimization Utility

We define the utility of a reasoning step based on its contribution to optimizing a target objective. For clarity, we omit the sample index i when discussing a single sample $z = (x, \mathbf{s}, a)$. Let \mathcal{T}_k denote the token set of step s_k , and write $L_k(\theta; z) = L(\theta; z, \mathcal{T}_k)$. We adopt a standard first-order influence perspective [14, 15]. Consider a small update induced by step s_k :

$$\theta' = \theta - \eta \nabla_\theta L_k(\theta; z), \quad (3)$$

where $\eta > 0$ is the learning rate. Let $L^{\text{tar}}(\theta; z)$ denote a target loss specifying the desired optimization direction; under Eq. 3, its first-order change is approximated as

$$\begin{aligned} L^{\text{tar}}(\theta'; z) - L^{\text{tar}}(\theta; z) &\approx -\eta \langle \nabla_\theta L_k, \nabla_\theta L^{\text{tar}} \rangle \\ &= -\eta \|\nabla_\theta L_k\| \|\nabla_\theta L^{\text{tar}}\| \cos(\nabla_\theta L_k, \nabla_\theta L^{\text{tar}}). \end{aligned} \quad (4)$$

This shows that a step is locally beneficial when its induced gradient is directionally aligned with the target gradient. Since step lengths and gradient scales can vary substantially across reasoning segments, we focus on the normalized directional component:

$$A_k^{\text{tar}} \triangleq \cos(\nabla_\theta L_k, \nabla_\theta L^{\text{tar}}). \quad (5)$$

See Appendix B for details. Different choices of target direction correspond to different notions of step utility. In GRACE, we consider two complementary objectives:

(1) Answer-oriented objective. We instantiate $L^{\text{tar}} = L^{\text{ans}}$, where $L^{\text{ans}}(\theta; z) = L(\theta; z, \mathcal{T}_{\text{ans}})$ is the loss on the answer segment and \mathcal{T}_{ans} denotes its token set. This gives

$$A_k^{\text{ans}} \triangleq \cos(\nabla_\theta L_k, \nabla_\theta L^{\text{ans}}). \quad (6)$$

which measures whether the step supports optimizing the final answer. While the answer-oriented objective captures whether a step supports the final answer, it does not characterize whether the step is coherent with the reasoning process that precedes it.

(2) Trajectory consistency objective. Reasoning steps form an ordered trajectory rather than independent supervision signals. For steps with preceding context, we define the historical reference direction and its corresponding alignment score jointly:

$$A_k^{\text{hist}} \triangleq \cos(\nabla_\theta L_k, r_k), \quad r_k \triangleq \text{Normalize} \left(\sum_{j < k} \omega_{k,j} \nabla_\theta L_j \right), \quad (7)$$

where $\omega_{k,j} \geq 0$ and $\sum_{j < k} \omega_{k,j} = 1$ control the contribution of each previous step to the historical reference direction. The score A_k^{hist} measures whether the current step continues the existing reasoning trajectory.

Combining these two criteria, the final step-level utility is defined as

$$\text{Score}_k \triangleq \alpha A_k^{\text{ans}} + (1 - \alpha) A_k^{\text{hist}}, \quad \alpha \in [0, 1], \quad (8)$$

where the historical term is omitted for $k = 1$, since no preceding context exists.

2.3 Representation-level Gradient Proxy

The step utility in Eq. 8 is defined through parameter-space gradients. Directly evaluating such gradients for every reasoning step would require isolating each step as a separate loss and performing repeated backward passes over decomposed traces. To obtain a scalable estimate of step-level alignment, we project the optimization signal to the final representation interface and compute alignment in this lower-dimensional space.

Since the full gradient can be decomposed as $\nabla_{\theta} L = [\nabla_{W_{\text{out}}} L; \nabla_{\theta_{\text{rep}}} L]$, we estimate step-induced directions in the representation-producing subspace θ_{rep} , where all reasoning tokens interact through the model’s internal features. Let $h_t \in \mathbb{R}^d$ denote the final-layer hidden state at token position t , where d is the hidden dimension, and let $W_{\text{out}} \in \mathbb{R}^{d \times V}$ be the output projection matrix, where V is the vocabulary size. The pre-softmax logit is $\ell_t = W_{\text{out}}^{\top} h_t \in \mathbb{R}^V$, and the next-token probability is $p_t = \text{softmax}(\ell_t)$. For the token-level cross-entropy loss L_t ,

$$\frac{\partial L_t}{\partial \ell_t} = p_t - y_t,$$

where y_t is the one-hot target token. The corresponding gradient at the representation interface is

$$u_t \triangleq \frac{\partial L_t}{\partial h_t} = W_{\text{out}}(p_t - y_t). \quad (9)$$

Let θ_{rep} denote the parameters that produce the final-layer representations, and define $J_t = \partial h_t / \partial \theta_{\text{rep}}$. By the chain rule, the representation-parameter gradient induced by token t is $\nabla_{\theta_{\text{rep}}} L_t = J_t^{\top} u_t$. Accordingly, for a token set \mathcal{T} , the corresponding segment gradient is $\nabla_{\theta_{\text{rep}}} L(\mathcal{T}) = |\mathcal{T}|^{-1} \sum_{t \in \mathcal{T}} J_t^{\top} u_t$. Thus, $\{u_t\}$ are the common upstream optimization signals that drive updates of the representation-producing parameters through the Jacobian mapping.

Eq. 5 requires the cosine alignment between the update directions induced by two token segments. For two token sets \mathcal{T}_1 and \mathcal{T}_2 , its representation-parameter form is

$$\cos(\nabla_{\theta_{\text{rep}}} L(\mathcal{T}_1), \nabla_{\theta_{\text{rep}}} L(\mathcal{T}_2)) = \frac{\sum_{t \in \mathcal{T}_1} \sum_{t' \in \mathcal{T}_2} u_t^{\top} (J_t J_{t'}^{\top}) u_{t'}}{\left\| \sum_{t \in \mathcal{T}_1} J_t^{\top} u_t \right\| \left\| \sum_{t' \in \mathcal{T}_2} J_{t'}^{\top} u_{t'} \right\|}. \quad (10)$$

Eq. 10 shows that exact representation-parameter alignment depends on both token-level upstream signals and Jacobian-induced interactions $J_t J_{t'}^{\top}$.

Exact step-level evaluation of these interactions would require isolating each step loss and backpropagating it through θ_{rep} , leading to repeated per-step gradient computation. To make step-level scoring scalable, we introduce an interface-level surrogate that preserves upstream optimization signals while avoiding explicit construction of the Jacobian-induced geometry. This design follows scalable data valuation methods that approximate gradient information in proxy spaces [12, 16, 17]. Under this surrogate, the segment-level update direction is represented by the aggregated upstream signal:

$$g(\mathcal{T}) \triangleq \frac{1}{|\mathcal{T}|} \sum_{t \in \mathcal{T}} u_t. \quad (11)$$

The averaging follows the definition of the segment loss $L(\theta; z, \mathcal{T})$ as a token-level mean, ensuring that proxy directions are not biased by segment length.

Using the token sets \mathcal{T}_k and \mathcal{T}_{ans} , we write $g_k \triangleq g(\mathcal{T}_k)$ and $g_{\text{ans}} \triangleq g(\mathcal{T}_{\text{ans}})$. The step-level utility is then computed in the proxy space as

$$\widehat{\text{Score}}_k = \begin{cases} \widehat{A}_k^{\text{ans}}, & k = 1, \\ \alpha \widehat{A}_k^{\text{ans}} + (1 - \alpha) \widehat{A}_k^{\text{hist}}, & k > 1, \end{cases} \quad (12)$$

Table 1: Performance of Qwen3-VL-2B under the data selection methods. *Data %* denotes the proportion of training data used, and *Rel. Avg.* is the average relative performance over benchmarks. \uparrow indicates larger is better. **Bold** and underlined values denote the best and second-best results among 20% data selection methods, respectively.

Method	Data %	Hallusion[18] \uparrow	SQA[19] \uparrow	MMBench[20] \uparrow	MME[21] \uparrow		MMT[22] \uparrow		MathVista[23] \uparrow	MathVision[24] \uparrow		Rel. Avg. \uparrow
					Perc.	Cog.	SI	MI		MINI	Full	
Full	100%	43.7	80.2	69.3	1517.3	656.1	55.0	53.4	52.5	16.4	14.7	–
Random	20%	45.5	<u>84.5</u>	72.6	1495.5	653.2	57.4	54.8	52.3	16.4	13.9	101.4
Longest	20%	46.3	83.0	73.6	1494.5	687.5	56.4	54.6	51.3	15.8	14.5	101.7
Stepmax	20%	46.9	83.8	<u>73.7</u>	1477.7	637.5	56.7	54.5	52.6	15.5	15.1	101.5
LESS [12]	20%	44.6	83.1	70.2	<u>1511.4</u>	668.6	56.0	53.7	49.9	<u>18.8</u>	14.3	101.7
ICONS [7]	20%	46.3	82.6	71.5	1497.0	675.0	55.5	53.8	51.0	13.2	14.4	99.1
CADC [13]	20%	44.6	84.4	73.1	1498.9	630.7	<u>57.5</u>	<u>55.2</u>	<u>54.0</u>	16.1	<u>16.1</u>	<u>102.6</u>
GRACE	5%	48.5	83.0	71.1	1509.3	617.5	56.5	55.1	51.9	14.0	14.8	100.2
	10%	45.7	82.5	69.5	1500.7	660.4	57.7	55.1	53.0	18.1	15.5	103.2
(Ours)	15%	48.5	82.6	71.1	1500.5	679.3	57.6	54.9	54.3	17.8	16.7	105.2
	20%	<u>46.8</u>	85.0	73.8	1512.3	<u>682.9</u>	58.5	56.3	54.2	21.7	17.2	108.8

where

$$\hat{A}_k^{\text{ans}} \triangleq \cos(g_k, g_{\text{ans}}), \quad \hat{A}_k^{\text{hist}} \triangleq \cos(g_k, \hat{r}_k), \quad \hat{r}_k \triangleq \text{Normalize} \left(\sum_{j < k} \omega_{k,j} g_j \right).$$

Importantly, for each sample, the fixed output projection W_{out} , the forward-pass probabilities $\{p_t\}$, and the ground-truth tokens $\{y_t\}$ are sufficient to obtain directional gradient proxies for all reasoning steps in a single forward pass, without constructing per-step training instances or performing backward passes. Detailed derivation is provided in Appendix C.

2.4 Sample-level Aggregation

Given the step-level proxy utility $\widehat{\text{Score}}_{i,k}$ in Eq. 12, GRACE instantiates the sample value $V(z_i)$ by averaging step-level utilities:

$$V(z_i) = \frac{1}{K_i} \sum_{k=1}^{K_i} \widehat{\text{Score}}_{i,k}. \quad (13)$$

This aggregation treats the reasoning trace as a sequence of optimization events and measures its overall training value by the average step-level utility.

The samples are ranked by $V(z_i)$ and selected according to the top-budget rule in Eq. 2. The selected subset \mathcal{S} is used for post-training with the original reasoning traces. See Appendix D for details.

3 Experiments

We empirically validate GRACE through a series of experiments designed to answer five questions:

- Does GRACE curate reasoning data more effectively than existing methods (Sec. 3.1)?
- Do the curated subsets transfer across model backbones (Sec. 3.2)?
- Which components of GRACE drive its effectiveness (Sec. 3.3)?
- How robust is GRACE to its design hyperparameters (Sec. 3.4)?
- What is the computational cost of GRACE relative to gradient-based alternatives (Sec. 3.5)?

Experimental Setup. We evaluate GRACE by post-training Qwen3-VL-2B-Instruct on the reasoning-rich candidate pool of MMathCoT-1M and comparing against heuristic selectors (Random, Longest, Stepmax) and data-curation baselines (LESS, ICONS, CADC) under the same selection budget and training recipe. Evaluation covers general VQA/perception, multi-task and multi-image reasoning, and mathematical reasoning benchmarks, with *Rel. Avg.* denoting performance normalized by the full-data baseline. Unless otherwise stated, GRACE uses $\rho = 0.2$, $\gamma = 0.05$, uniform history aggregation, and $\alpha = 0.7$. Full experimental details, including datasets, backbones, benchmarks, training recipes, and hardware, are provided in Appendix E.

Table 2: Relative average performance (%) of Qwen3-VL-2B under different data selection ratios. *Data %* denotes the proportion of data used. Values are normalized to the full-data training baseline.

Data %	Full	Random	Longest	Stepmax	LESS	ICONS	CADC	GRACE (Ours)
5%	100.0	96.4	98.3	95.6	90.4	95.9	99.8	100.2
10%	100.0	98.5	100.5	98.8	95.5	<u>102.4</u>	101.3	103.2
15%	100.0	100.0	98.2	100.6	98.9	<u>101.7</u>	100.7	105.2

3.1 Main Results

Table 1 reports per-benchmark performance on Qwen3-VL-2B, comparing all baselines at a 20% selection ratio against GRACE at 5%, 10%, 15%, and 20%. GRACE consistently outperforms all heuristic and gradient-based baselines: at 20% data, it reaches 108.8% relative average, surpassing the strongest baseline (CADC, 102.6%) by a substantial margin and exceeding the full-data baseline by 8.8 points. With only 5% of the data, GRACE retains 100.2% of full-data performance, demonstrating that step-level optimization-aware scoring can identify highly compact yet informative subsets. This gain over full-data training is partly due to continued SFT on an instruction-tuned backbone: the math-centric candidate pool may over-specialize the model toward mathematical reasoning and cause partial forgetting on general VQA and perception abilities. Thus, reduced subsets can sometimes outperform full-data SFT, while GRACE further improves this effect by selecting traces with more favorable step-level optimization signals.

Table 2 compares relative average performance across 5%–15% selection ratios. GRACE is the only method that exceeds full-data performance at every ratio, while heuristic baselines fluctuate around the full-data line and gradient-based baselines are unstable at low ratios.

3.2 Transfer Across Backbones

To test whether the value assigned by GRACE reflects data properties that transfer beyond the scoring backbone, we post-train other backbones on the subset selected using Qwen3-VL-2B, *without* re-running data selection. We consider Qwen2.5-VL-3B [25], LLaVA-1.5-7B [26], and Qwen3-VL-8B [11], covering different model families and scales, and compare them with their corresponding full-data baselines under the same training recipe.

Figure 3 further examines whether GRACE-selected data transfer across backbones. The line reports the relative average performance of the 20% GRACE subset, normalized by each backbone’s full-data baseline. The dashed horizontal line marks the 100% full-data level, and the bars compare single-GPU wall-clock training time under 100% and 20% data. We select the 20% subset once using Qwen3-VL-2B and reuse it to post-train Qwen2.5-VL-3B, LLaVA-1.5-7B, and Qwen3-VL-8B without re-running data selection. The curated subset consistently surpasses the corresponding full-data baseline across all backbones, indicating that the value captured by GRACE is not tied to a single scoring model. This suggests that step-level optimization utility reflects transferable properties of reasoning data rather than model-specific artifacts.

In addition to transferability, the selected subset substantially reduces training cost, with larger savings on larger backbones where full-data post-training is more expensive. Overall, GRACE improves the efficiency–performance trade-off: a compact reasoning subset can match or surpass full-data performance while requiring only a fraction of the training time.

3.3 Ablation Studies

We ablate the two utility components and gradient proxy on Qwen3-VL-2B at $\rho = 0.2$. We consider five variants: (a) **w/o historical score**: setting $\alpha = 1$, scoring each step only by answer-oriented alignment; (b) **w/o answer score**: removing the answer-oriented term and scoring steps only by

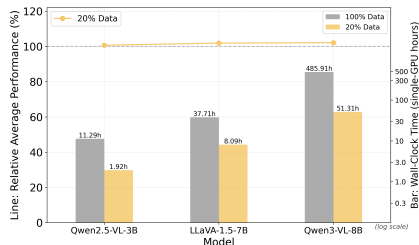


Figure 3: Transferability and training efficiency across backbones.

Table 3: Ablation study of GRACE on Qwen3-VL-2B at $\rho = 0.2$.

Variant	Hallusion \uparrow	SQA \uparrow	MMBench \uparrow	MME \uparrow		MMT \uparrow		MathVista \uparrow	MathVision \uparrow		Rel. Avg. \uparrow
				Perc.	Cog.	SI	MI		MINI	Full	
GRACE	46.8	85.0	73.8	<u>1512.3</u>	<u>682.9</u>	58.5	56.3	<u>54.2</u>	21.7	<u>17.2</u>	108.8
w/o Hist.	45.9	83.3	71.0	1502.6	686.8	56.6	<u>54.8</u>	55.2	<u>17.2</u>	18.4	<u>105.5</u>
w/o Ans.	44.5	80.8	69.7	1495.1	655.4	55.2	53.3	50.7	13.6	13.8	97.5
Target = CoT + Ans	46.8	81.8	69.2	1508.1	655.0	56.1	54.5	50.7	15.3	14.5	100.2
Target = Suffix	44.4	82.1	68.5	1515.9	656.1	55.2	52.7	51.3	14.4	15.1	99.0
Proxy = Proj. Grad.	45.7	82.9	<u>71.7</u>	1501.0	661.8	<u>56.7</u>	<u>54.8</u>	49.0	12.7	14.1	98.3

Table 4: Hyperparameter analysis on Qwen3-VL-2B at $\rho = 0.2$. γ denotes the warm-up ratio; W and β are used for window and EMA history aggregation, respectively. For four-checkpoint scoring, 0.25–1.0 denotes checkpoints at 25%, 50%, 75%, and 100% warm-up progress.

Study	Variant	γ	Hist.	W	β	α	Rel. Avg. \uparrow
Pool	≥ 8 -step	–	–	–	–	–	100.0
	Full w/o filter	–	–	–	–	–	99.3
Warm-up	No warm-up	0	uniform	–	–	0.5	89.6
	Larger warm-up	0.25	uniform	–	–	0.5	99.6
	Four checkpoints	0.25–1.0	uniform	–	–	0.5	101.7
	Default	0.05	uniform	–	–	0.5	106.6
History	Window	0.05	window	3	–	0.5	104.6
	EMA	0.05	EMA	–	0.8	0.5	105.7
	Uniform	0.05	uniform	–	–	0.5	106.6
Balance	$\alpha = 0.1$	0.05	uniform	–	–	0.1	100.8
	$\alpha = 0.5$	0.05	uniform	–	–	0.5	106.6
	$\alpha = 0.7$ (default)	0.05	uniform	–	–	0.7	108.8
	$\alpha = 0.9$	0.05	uniform	–	–	0.9	<u>107.7</u>

historical alignment, with the first step omitted since no history exists; (c) **Target = CoT + Ans**: using the union of all reasoning steps and the answer as the optimization target; (d) **Target = Suffix**: using the trailing suffix after the current step, testing whether local future context suffices as an answer surrogate; (e) **Proxy = projected gradient**: replacing $g(\mathcal{T})$ with LESS-style projected parameter-space gradients computed per step, while keeping the rest of GRACE unchanged.

Table 3 reports the ablation results across all benchmarks. Both utility components contribute to GRACE. Using only answer-oriented alignment remains competitive, reaching 105.5% relative average performance, but still trails full GRACE by 3.3 points, showing that trajectory consistency provides complementary information beyond answer alignment. In contrast, removing the answer-oriented term drops the relative average to 97.5%, suggesting that historical consistency alone may favor internally coherent traces that are not necessarily aligned with the final optimization objective.

The target direction also matters. Replacing the answer segment with the full trace (*CoT + Ans*) or local suffix reduces the relative average to 100.2% and 99.0%, respectively, indicating that the final answer is a more reliable target for step-level utility estimation. Finally, replacing our representation-level proxy with projected parameter-space gradients yields only 98.3%, confirming that our proxy is not merely an efficiency approximation but also provides a stable signal for reasoning-step valuation.

3.4 Hyperparameter Analysis

We study the sensitivity of GRACE to its main hyperparameters on Qwen3-VL-2B at $\rho = 0.2$. We examine: (i) the candidate pool (default ≥ 8 -step subset of MMathCoT-1M vs. full MMathCoT-1M); (ii) the warm-up strategy, including the warm-up ratio γ and scoring checkpoints; (iii) the history aggregation scheme $\omega_{k,j}$ (uniform / sliding window with size W / EMA with decay β); and (iv) the balance coefficient $\alpha \in [0, 1]$ for answer-oriented and historical alignment.

Table 4 summarizes representative hyperparameter variants. These results lead to four main observations. **Candidate pool.** The ≥ 8 -step pool slightly outperforms the unfiltered MMathCoT-1M

Table 5: Cost complexity of feature/signal collection.

Method	Time Complexity	Storage Complexity
Gradient projection	$\mathcal{O}(M(\mathcal{D}_{\text{train}} + \mathcal{D}_{\text{target}})(C_{\text{fwd}} + C_{\text{bwd}}))$	$\mathcal{O}(M(\mathcal{D}_{\text{train}} + \mathcal{D}_{\text{target}})d_{\text{proj}})$
GRACE gradient proxy	$\mathcal{O}(M \mathcal{D}_{\text{train}} C_{\text{fwd}})$	$\mathcal{O}(M \mathcal{D}_{\text{train}} (K + 1)d)$

pool, supporting the use of reasoning-rich traces for stable step-level scoring. **Warm-up.** Without warm-up, performance drops to 89.6%, while the lightweight default warm-up with $\gamma = 0.05$ reaches 106.6%, outperforming larger warm-up or multi-checkpoint scoring. **History aggregation.** Uniform cumulative averaging performs best among the tested strategies, suggesting that broader reasoning history provides a stable reference direction. **Balance coefficient.** $\alpha = 0.7$ achieves the best result (108.8%), showing that answer alignment should dominate while still retaining trajectory consistency. Full per-benchmark results are provided in Appendix F.

3.5 Computational Cost

We focus on the dominant offline cost of feature/signal collection, as the subsequent ranking and top- ρ selection costs are negligible in comparison. Let $\mathcal{D}_{\text{train}}$ and $\mathcal{D}_{\text{target}}$ denote the candidate pool and the target/validation set, respectively; let M be the number of scoring checkpoints, K the average number of reasoning steps, d_{proj} the projected-gradient dimension, and d the hidden dimension defined in Sec. 2.3. We use C_{fwd} and C_{bwd} for the cost of one forward and backward pass. Table 5 summarizes the time and storage complexity of this collection stage.

Gradient-projection methods collect projected gradients for both training and target samples, and each feature requires a forward-backward pass. This is expensive because it scales with both $\mathcal{D}_{\text{train}}$ and $\mathcal{D}_{\text{target}}$ and stores d_{proj} -dimensional gradients for all samples. GRACE simplifies this collection stage. It requires no target set or backward computation; instead, it only performs forward passes over candidate training samples. Token-level upstream signals are then grouped into K step proxies and one answer proxy in the hidden dimension d , enabling step-aware valuation in a single pass per sample. In practice, this proxy collection remains lightweight, taking 6.5 single-node hours and 5.7GB of storage on the candidate pool.

Overall, GRACE replaces backward-based gradient extraction with forward-only proxy collection, making step-level reasoning data valuation substantially more efficient while preserving the fine-grained structure needed for our scoring objective.

4 Related Work

Reasoning supervision and step-level evaluation. Chain-of-thought prompting and supervision improve reasoning by exposing intermediate rationales [1, 2]. As reasoning datasets scale, post-training pipelines often curate data using quality indicators, such as final-answer correctness, self-consistency [5], reward-model scores, or preference signals [6, 27]. Process-supervision methods further evaluate intermediate steps with human annotations or verifiers [3, 10, 28, 29]. GRACE instead scores steps with internal optimization signals, without external rewards or step annotations.

Data valuation and efficient post-training. Influence functions and TracIn-style estimators measure training-sample effects through optimization dynamics [14, 15, 30, 31], and scalable variants such as LESS approximate these effects with projected gradients [12, 32]. Vision-language data selection methods further explore influence consensus or capability-aware curation [7, 13], while efficient instruction tuning often relies on diversity [33], difficulty [34], task coverage [7], data quality [8, 35–37], or sample-level influence [7, 12, 13]. These methods mainly operate at the sample level, whereas GRACE models the ordered internal structure of reasoning traces and aggregates step-level directional utilities for subset selection.

5 Conclusion

We present GRACE, a gradient-aligned reasoning data curation method for efficient post-training. Instead of treating a reasoning trace as an indivisible supervision unit, GRACE views it as a sequence

of optimization events and evaluates each step through answer-oriented alignment and trajectory consistency. To make this fine-grained valuation scalable, we introduce a representation-level gradient proxy that estimates step-induced update directions from forward-pass upstream signals, avoiding per-step backward computation. Experiments on multimodal reasoning post-training show that GRACE selects compact subsets that match or surpass full-data training, with 20% curated data reaching 108.8% of full-data performance and 5% retaining 100.2%. These results suggest that the value of reasoning data depends not only on external quality indicators such as correctness, preference, or length, but also on whether its intermediate steps constructively support the optimization trajectory.

References

- [1] Jason Wei, Xuezhi Wang, Dale Schuurmans, Maarten Bosma, brian ichter, Fei Xia, Ed Chi, Quoc V Le, and Denny Zhou. Chain-of-thought prompting elicits reasoning in large language models. In S. Koyejo, S. Mohamed, A. Agarwal, D. Belgrave, K. Cho, and A. Oh, editors, *Advances in Neural Information Processing Systems*, volume 35, pages 24824–24837. Curran Associates, Inc., 2022. URL https://proceedings.neurips.cc/paper_files/paper/2022/file/9d5609613524ecf4f15af0f7b31abca4-Paper-Conference.pdf.
- [2] Guowei Xu, Peng Jin, Hao Li, Yibing Song, Lichao Sun, and Li Yuan. Llava-cot: Let vision language models reason step-by-step. *CoRR*, abs/2411.10440, 2024. doi: 10.48550/ARXIV.2411.10440. URL <https://doi.org/10.48550/arXiv.2411.10440>.
- [3] Ruilin Luo, Zhuofan Zheng, Lei Wang, Yifan Wang, Xinzhe Ni, Zicheng Lin, Songtao Jiang, Yiyao Yu, Chufan Shi, Ruihang Chu, Jin zeng, and Yujiu Yang. Unlocking multimodal mathematical reasoning via process reward model. In D. Belgrave, C. Zhang, H. Lin, R. Pascanu, P. Koniusz, M. Ghassemi, and N. Chen, editors, *Advances in Neural Information Processing Systems*, volume 38, pages 49851–49899. Curran Associates, Inc., 2025. URL https://proceedings.neurips.cc/paper_files/paper/2025/file/4757e472d97ca980c24a487622f7ff00-Paper-Conference.pdf.
- [4] Chunting Zhou, Pengfei Liu, Puxin Xu, Srinivasan Iyer, Jiao Sun, Yuning Mao, Xuezhe Ma, Avia Efrat, Ping Yu, Lili Yu, Susan Zhang, Gargi Ghosh, Mike Lewis, Luke Zettlemoyer, and Omer Levy. LIMA: less is more for alignment. In Alice Oh, Tristan Naumann, Amir Globerson, Kate Saenko, Moritz Hardt, and Sergey Levine, editors, *Advances in Neural Information Processing Systems 36: Annual Conference on Neural Information Processing Systems 2023, NeurIPS 2023, New Orleans, LA, USA, December 10 - 16, 2023*, 2023. URL http://papers.nips.cc/paper_files/paper/2023/hash/ac662d74829e4407ce1d126477f4a03a-Abstract-Conference.html.
- [5] Xuezhi Wang, Jason Wei, Dale Schuurmans, Quoc V. Le, Ed H. Chi, Sharan Narang, Aakanksha Chowdhery, and Denny Zhou. Self-consistency improves chain of thought reasoning in language models. In *The Eleventh International Conference on Learning Representations, ICLR 2023, Kigali, Rwanda, May 1-5, 2023*. OpenReview.net, 2023. URL <https://openreview.net/forum?id=1PL1NIMMrw>.
- [6] Long Ouyang, Jeffrey Wu, Xu Jiang, Diogo Almeida, Carroll L. Wainwright, Pamela Mishkin, Chong Zhang, Sandhini Agarwal, Katarina Slama, Alex Ray, John Schulman, Jacob Hilton, Fraser Kelton, Luke Miller, Maddie Simens, Amanda Askell, Peter Welinder, Paul F. Christiano, Jan Leike, and Ryan Lowe. Training language models to follow instructions with human feedback. In Sanmi Koyejo, S. Mohamed, A. Agarwal, Danielle Belgrave, K. Cho, and A. Oh, editors, *Advances in Neural Information Processing Systems 35: Annual Conference on Neural Information Processing Systems 2022, NeurIPS 2022, New Orleans, LA, USA, November 28 - December 9, 2022*, 2022. URL http://papers.nips.cc/paper_files/paper/2022/hash/b1efde53be364a73914f58805a001731-Abstract-Conference.html.
- [7] Xindi Wu, Mengzhou Xia, Rulin Shao, Zhiwei Deng, Pang Wei Koh, and Olga Russakovsky. ICONS: influence consensus for vision-language data selection. *CoRR*, abs/2501.00654, 2025.
- [8] Zikang Liu, Kun Zhou, Wayne Xin Zhao, Dawei Gao, Yaliang Li, and Ji-Rong Wen. Less is more: High-value data selection for visual instruction tuning. *CoRR*, abs/2403.09559, 2024.

- [9] Jaewoo Lee, Boyang Li, and Sung Ju Hwang. Concept-skill transferability-based data selection for large vision-language models. In Yaser Al-Onaizan, Mohit Bansal, and Yun-Nung Chen, editors, *Proceedings of the 2024 Conference on Empirical Methods in Natural Language Processing, EMNLP 2024, Miami, FL, USA, November 12-16, 2024*, pages 5060–5080, 2024.
- [10] Jonathan Uesato, Nate Kushman, Ramana Kumar, H. Francis Song, Noah Y. Siegel, Lisa Wang, Antonia Creswell, Geoffrey Irving, and Irina Higgins. Solving math word problems with process- and outcome-based feedback. *CoRR*, abs/2211.14275, 2022. doi: 10.48550/ARXIV.2211.14275. URL <https://doi.org/10.48550/arXiv.2211.14275>.
- [11] Qwen Team. Qwen3-v1 technical report. *CoRR*, abs/2511.21631, 2025. doi: 10.48550/ARXIV.2511.21631. URL <https://doi.org/10.48550/arXiv.2511.21631>.
- [12] Mengzhou Xia, Sadhika Malladi, Suchin Gururangan, Sanjeev Arora, and Danqi Chen. LESS: selecting influential data for targeted instruction tuning. In *Forty-first International Conference on Machine Learning, ICML 2024, Vienna, Austria, July 21-27, 2024*. OpenReview.net, 2024.
- [13] Junjie Li, Ziao Wang, Jianghong Ma, and Xiaofeng Zhang. Uncovering intrinsic capabilities: A paradigm for data curation in vision-language models. *CoRR*, abs/2510.00040, 2025. doi: 10.48550/ARXIV.2510.00040. URL <https://doi.org/10.48550/arXiv.2510.00040>.
- [14] Garima Pruthi, Frederick Liu, Satyen Kale, and Mukund Sundararajan. Estimating training data influence by tracing gradient descent. In Hugo Larochelle, Marc’Aurelio Ranzato, Raia Hadsell, Maria-Florina Balcan, and Hsuan-Tien Lin, editors, *Advances in Neural Information Processing Systems 33: Annual Conference on Neural Information Processing Systems 2020, NeurIPS 2020, December 6-12, 2020, virtual*, 2020.
- [15] Pang Wei Koh and Percy Liang. Understanding black-box predictions via influence functions. In Doina Precup and Yee Whye Teh, editors, *Proceedings of the 34th International Conference on Machine Learning, ICML 2017, Sydney, NSW, Australia, 6-11 August 2017*, Proceedings of Machine Learning Research, pages 1885–1894. PMLR, 2017. URL <http://proceedings.mlr.press/v70/koh17a.html>.
- [16] Jordan T. Ash, Chicheng Zhang, Akshay Krishnamurthy, John Langford, and Alekh Agarwal. Deep batch active learning by diverse, uncertain gradient lower bounds. In *8th International Conference on Learning Representations, ICLR 2020, Addis Ababa, Ethiopia, April 26-30, 2020*. OpenReview.net, 2020. URL <https://openreview.net/forum?id=ryghZJBKPS>.
- [17] Sung Min Park, Kristian Georgiev, Andrew Ilyas, Guillaume Leclerc, and Aleksander Madry. TRAK: attributing model behavior at scale. In Andreas Krause, Emma Brunskill, Kyunghyun Cho, Barbara Engelhardt, Sivan Sabato, and Jonathan Scarlett, editors, *International Conference on Machine Learning, ICML 2023, 23-29 July 2023, Honolulu, Hawaii, USA*, Proceedings of Machine Learning Research, pages 27074–27113. PMLR, 2023. URL <https://proceedings.mlr.press/v202/park23c.html>.
- [18] Tianrui Guan, Fuxiao Liu, Xiyang Wu, Ruiqi Xian, Zongxia Li, Xiaoyu Liu, Xijun Wang, Lichang Chen, Furong Huang, Yaser Yacoub, Dinesh Manocha, and Tianyi Zhou. Hallusionbench: An advanced diagnostic suite for entangled language hallucination and visual illusion in large vision-language models. In *IEEE/CVF Conference on Computer Vision and Pattern Recognition, CVPR 2024, Seattle, WA, USA, June 16-22, 2024*, pages 14375–14385. IEEE, 2024. doi: 10.1109/CVPR52733.2024.01363. URL <https://doi.org/10.1109/CVPR52733.2024.01363>.
- [19] Pan Lu, Swaroop Mishra, Tanglin Xia, Liang Qiu, Kai-Wei Chang, Song-Chun Zhu, Oyvind Tafjord, Peter Clark, and Ashwin Kalyan. Learn to explain: Multimodal reasoning via thought chains for science question answering. In Sanmi Koyejo, S. Mohamed, A. Agarwal, Danielle Belgrave, K. Cho, and A. Oh, editors, *Advances in Neural Information Processing Systems 35: Annual Conference on Neural Information Processing Systems 2022, NeurIPS 2022, New Orleans, LA, USA, November 28 - December 9, 2022*. URL http://papers.nips.cc/paper_files/paper/2022/hash/11332b6b6cf4485b84afadb1352d3a9a-Abstract-Conference.html.

- [20] Yuan Liu, Haodong Duan, Yuanhan Zhang, Bo Li, Songyang Zhang, Wangbo Zhao, Yike Yuan, Jiaqi Wang, Conghui He, Ziwei Liu, Kai Chen, and Dahua Lin. Mmbench: Is your multi-modal model an all-around player? In Ales Leonardis, Elisa Ricci, Stefan Roth, Olga Russakovsky, Torsten Sattler, and Gül Varol, editors, *Computer Vision - ECCV 2024 - 18th European Conference, Milan, Italy, September 29-October 4, 2024, Proceedings, Part VI*, Lecture Notes in Computer Science, pages 216–233. Springer, 2024. doi: 10.1007/978-3-031-72658-3_13. URL https://doi.org/10.1007/978-3-031-72658-3_13.
- [21] Chaoyou Fu, Peixian Chen, Yunhang Shen, Yulei Qin, Mengdan Zhang, Xu Lin, Zhenyu Qiu, Wei Lin, Jinrui Yang, Xiawu Zheng, Ke Li, Xing Sun, and Rongrong Ji. MME: A comprehensive evaluation benchmark for multimodal large language models. *CoRR*, abs/2306.13394, 2023. doi: 10.48550/ARXIV.2306.13394. URL <https://doi.org/10.48550/arXiv.2306.13394>.
- [22] Kaining Ying, Fanqing Meng, Jin Wang, Zhiqian Li, Han Lin, Yue Yang, Hao Zhang, Wenbo Zhang, Yuqi Lin, Shuo Liu, Jiayi Lei, Quanfeng Lu, Runjian Chen, Peng Xu, Renrui Zhang, Haozhe Zhang, Peng Gao, Yali Wang, Yu Qiao, Ping Luo, Kaipeng Zhang, and Wenqi Shao. Mmt-bench: A comprehensive multimodal benchmark for evaluating large vision-language models towards multitask AGI. In Ruslan Salakhutdinov, Zico Kolter, Katherine A. Heller, Adrian Weller, Nuria Oliver, Jonathan Scarlett, and Felix Berkenkamp, editors, *Forty-first International Conference on Machine Learning, ICML 2024, Vienna, Austria, July 21-27, 2024*, Proceedings of Machine Learning Research, pages 57116–57198. PMLR / OpenReview.net, 2024. URL <https://proceedings.mlr.press/v235/ying24a.html>.
- [23] Pan Lu, Hritik Bansal, Tony Xia, Jiacheng Liu, Chunyuan Li, Hannaneh Hajishirzi, Hao Cheng, Kai-Wei Chang, Michel Galley, and Jianfeng Gao. Mathvista: Evaluating mathematical reasoning of foundation models in visual contexts. In *The Twelfth International Conference on Learning Representations, ICLR 2024, Vienna, Austria, May 7-11, 2024*. OpenReview.net, 2024. URL <https://openreview.net/forum?id=KUNzEQMWU7>.
- [24] Ke Wang, Junting Pan, Weikang Shi, Zimu Lu, Houxing Ren, Aojun Zhou, Mingjie Zhan, and Hongsheng Li. Measuring multimodal mathematical reasoning with math-vision dataset. In Amir Globersons, Lester Mackey, Danielle Belgrave, Angela Fan, Ulrich Paquet, Jakub M. Tomczak, and Cheng Zhang, editors, *Advances in Neural Information Processing Systems 38: Annual Conference on Neural Information Processing Systems 2024, NeurIPS 2024, Vancouver, BC, Canada, December 10 - 15, 2024*, 2024. URL http://papers.nips.cc/paper_files/paper/2024/hash/ad0edc7d5fa1a783f063646968b7315b-Abstract-Datasets_and_Benchmarks_Track.html.
- [25] Qwen Team. Qwen2.5-vl, January 2025. URL <https://qwenlm.github.io/blog/qwen2.5-vl/>.
- [26] Haotian Liu, Chunyuan Li, Yuheng Li, and Yong Jae Lee. Improved baselines with visual instruction tuning. In *IEEE/CVF Conference on Computer Vision and Pattern Recognition, CVPR 2024, Seattle, WA, USA, June 16-22, 2024*, pages 26286–26296. IEEE, 2024. doi: 10.1109/CVPR52733.2024.02484. URL <https://doi.org/10.1109/CVPR52733.2024.02484>.
- [27] Rafael Rafailov, Archit Sharma, Eric Mitchell, Christopher D. Manning, Stefano Ermon, and Chelsea Finn. Direct preference optimization: Your language model is secretly a reward model. In Alice Oh, Tristan Naumann, Amir Globerson, Kate Saenko, Moritz Hardt, and Sergey Levine, editors, *Advances in Neural Information Processing Systems 36: Annual Conference on Neural Information Processing Systems 2023, NeurIPS 2023, New Orleans, LA, USA, December 10 - 16, 2023*, 2023. URL http://papers.nips.cc/paper_files/paper/2023/hash/a85b405ed65c6477a4fe8302b5e06ce7-Abstract-Conference.html.
- [28] Hunter Lightman, Vineet Kosaraju, Yura Burda, Harri Edwards, Bowen Baker, Teddy Lee, Jan Leike, John Schulman, Ilya Sutskever, and Karl Cobbe. Let’s verify step by step, 2023. URL <https://arxiv.org/abs/2305.20050>.
- [29] Minghe Gao, Xuqi Liu, Zhongqi Yue, Yang Wu, Shuang Chen, Juncheng Li, Siliang Tang, Fei Wu, Tat-Seng Chua, and Yueting Zhuang. Benchmarking Multimodal CoT Reward Model Step-wise by Visual Program. In *International Conference on Computer Vision*, pages 1718–1728, 2025. URL <https://mlanthology.org/iccv/2025/gao2025iccv-benchmarking/>.

- [30] Chih-Kuan Yeh, Joon Kim, Ian En-Hsu Yen, and Pradeep K Ravikumar. Representer point selection for explaining deep neural networks. *Advances in neural information processing systems*, 31, 2018.
- [31] Amirata Ghorbani and James Y. Zou. Data shapley: Equitable valuation of data for machine learning. In Kamalika Chaudhuri and Ruslan Salakhutdinov, editors, *Proceedings of the 36th International Conference on Machine Learning, ICML 2019, 9-15 June 2019, Long Beach, California, USA*, Proceedings of Machine Learning Research, pages 2242–2251. PMLR, 2019. URL <http://proceedings.mlr.press/v97/ghorbani19c.html>.
- [32] Andrew Ilyas, Sung Min Park, Logan Engstrom, Guillaume Leclerc, and Aleksander Madry. Datamodels: Predicting predictions from training data. In *ICML, 2022*.
- [33] Shengguang Wu, Keming Lu, Benfeng Xu, Junyang Lin, Qi Su, and Chang Zhou. Self-evolved diverse data sampling for efficient instruction tuning. *CoRR*, abs/2311.08182, 2023. doi: 10.48550/ARXIV.2311.08182. URL <https://doi.org/10.48550/arXiv.2311.08182>.
- [34] Can Xu, Qingfeng Sun, Kai Zheng, Xiubo Geng, Pu Zhao, Jiazhan Feng, Chongyang Tao, Qingwei Lin, and Daxin Jiang. Wizardlm: Empowering large pre-trained language models to follow complex instructions. In B. Kim, Y. Yue, S. Chaudhuri, K. Fragkiadaki, M. Khan, and Y. Sun, editors, *International Conference on Learning Representations*, volume 2024, pages 30745–30766, 2024. URL https://proceedings.iclr.cc/paper_files/paper/2024/file/82eec786fdfbbfa53450c5feb7d1ac92-Paper-Conference.pdf.
- [35] Wei Liu, Weihao Zeng, Keqing He, Yong Jiang, and Junxian He. What makes good data for alignment? A comprehensive study of automatic data selection in instruction tuning. In *The Twelfth International Conference on Learning Representations, ICLR 2024, Vienna, Austria, May 7-11, 2024*. OpenReview.net, 2024. URL <https://openreview.net/forum?id=BTKAeLqLMw>.
- [36] Bardia Safaei, Faizan Siddiqui, Jiacong Xu, Vishal M. Patel, and Shao-Yuan Lo. Filter Images First, Generate Instructions Later: Pre-Instruction Data Selection for Visual Instruction Tuning. In *2025 IEEE/CVF Conference on Computer Vision and Pattern Recognition (CVPR)*, pages 14247–14256, Los Alamitos, CA, USA, June 2025. IEEE Computer Society. doi: 10.1109/CVPR52734.2025.01329. URL <https://doi.ieeecomputersociety.org/10.1109/CVPR52734.2025.01329>.
- [37] Yihan Cao, Yanbin Kang, Chi Wang, and Lichao Sun. Instruction mining: Instruction data selection for tuning large language models, 2024. URL <https://arxiv.org/abs/2307.06290>.
- [38] Yuze Zhao, Jintao Huang, Jinghan Hu, Xingjun Wang, Yunlin Mao, Daoze Zhang, Zeyinzi Jiang, Zhikai Wu, Baole Ai, Ang Wang, Wenmeng Zhou, and Yingda Chen. SWIFT: A scalable lightweight infrastructure for fine-tuning. In Toby Walsh, Julie Shah, and Zico Kolter, editors, *Thirty-Ninth AAAI Conference on Artificial Intelligence, Thirty-Seventh Conference on Innovative Applications of Artificial Intelligence, Fifteenth Symposium on Educational Advances in Artificial Intelligence, AAAI 2025, Philadelphia, PA, USA, February 25 - March 4, 2025*, pages 29733–29735. AAAI Press, 2025. doi: 10.1609/AAAI.V39I28.35383. URL <https://doi.org/10.1609/aaai.v39i28.35383>.
- [39] Haodong Duan, Junming Yang, Yuxuan Qiao, Xinyu Fang, Lin Chen, Yuan Liu, Xiaoyi Dong, Yuhang Zang, Pan Zhang, Jiaqi Wang, Dahua Lin, and Kai Chen. Vlmevalkit: An open-source toolkit for evaluating large multi-modality models. In Jianfei Cai, Mohan S. Kankanhalli, Balakrishnan Prabhakaran, Susanne Boll, Ramanathan Subramanian, Liang Zheng, Vivek K. Singh, Pablo César, Lexing Xie, and Dong Xu, editors, *Proceedings of the 32nd ACM International Conference on Multimedia, MM 2024, Melbourne, VIC, Australia, 28 October 2024 - 1 November 2024*, pages 11198–11201. ACM, 2024. doi: 10.1145/3664647.3685520. URL <https://doi.org/10.1145/3664647.3685520>.

A Limitations

GRACE has several limitations. First, GRACE estimates data utility from optimization signals observed under a fixed scoring model and warm-up configuration. Although our experiments show consistent gains across selection ratios, hyperparameter variants, and transferred backbones, applying GRACE to substantially different optimizers, training objectives, or model families may require additional empirical validation. Second, our empirical evaluation focuses on multimodal reasoning post-training with chain-of-thought data. While the results cover mathematical reasoning, general visual question answering, multi-task reasoning, and multi-image reasoning benchmarks, extending GRACE to pure language reasoning, non-CoT instruction data, or reinforcement-learning-based post-training remains an important direction for future work. Third, while improving data efficiency can reduce post-training cost and make reasoning model development more accessible, more effective curation may also lower the barrier to training stronger models for unintended or harmful downstream uses. This highlights the importance of responsible dataset governance, safety evaluation, and deployment when applying GRACE to capability-enhancing post-training pipelines.

B First-order Motivation for Directional Step Utility

For a sample z and a target loss $L^{\text{tar}}(\theta; z)$, consider the step-induced update

$$\theta' = \theta - \eta \nabla_{\theta} L_k(\theta; z), \quad (14)$$

where $\eta > 0$. Applying a first-order Taylor expansion at θ gives

$$L^{\text{tar}}(\theta'; z) = L^{\text{tar}}(\theta; z) + \langle \nabla_{\theta} L^{\text{tar}}(\theta; z), \theta' - \theta \rangle + O(\|\theta' - \theta\|^2) \quad (15)$$

$$= L^{\text{tar}}(\theta; z) - \eta \langle \nabla_{\theta} L^{\text{tar}}(\theta; z), \nabla_{\theta} L_k(\theta; z) \rangle + O(\eta^2). \quad (16)$$

Therefore,

$$L^{\text{tar}}(\theta'; z) - L^{\text{tar}}(\theta; z) = -\eta \langle \nabla_{\theta} L_k(\theta; z), \nabla_{\theta} L^{\text{tar}}(\theta; z) \rangle + O(\eta^2). \quad (17)$$

Under a small step size, ignoring the higher-order term yields Eq. 4.

The first-order term shows that the local effect of step s_k is governed by the inner product between the step gradient and the target gradient. This inner product can be written as

$$\langle \nabla_{\theta} L_k, \nabla_{\theta} L^{\text{tar}} \rangle = \|\nabla_{\theta} L_k\| \|\nabla_{\theta} L^{\text{tar}}\| A_k^{\text{tar}}, \quad (18)$$

where

$$A_k^{\text{tar}} \triangleq \cos(\nabla_{\theta} L_k, \nabla_{\theta} L^{\text{tar}}). \quad (19)$$

Thus, A_k^{tar} corresponds to the normalized directional component of the first-order utility. GRACE uses this normalized form to compare step directions while reducing the effect of gradient scale.

C Derivation of Representation-level Gradient Proxy

We derive the representation-level proxy in Sec. 2.3 from the parameter-space formulation in Sec. 2.2.

Let θ_{rep} denote the parameters that produce the final hidden representations. For a token-level loss L_t , by the chain rule,

$$\nabla_{\theta_{\text{rep}}} L_t = \left(\frac{\partial h_t}{\partial \theta_{\text{rep}}} \right)^{\top} \frac{\partial L_t}{\partial h_t} = J_t^{\top} u_t, \quad (20)$$

where

$$J_t \triangleq \frac{\partial h_t}{\partial \theta_{\text{rep}}}, \quad u_t \triangleq \frac{\partial L_t}{\partial h_t}.$$

For softmax cross-entropy, let $\ell_t = W_{\text{out}}^{\top} h_t$, $p_t = \text{softmax}(\ell_t)$, and y_t be the one-hot label. The token-level loss is

$$L_t = - \sum_{v=1}^V (y_t)_v \log p_{t,v}, \quad p_{t,v} = \frac{\exp(\ell_{t,v})}{\sum_{r=1}^V \exp(\ell_{t,r})}.$$

The derivative of the softmax probability with respect to the logit is

$$\frac{\partial p_{t,v}}{\partial \ell_{t,r}} = p_{t,v}(\mathbf{1}_{v=r} - p_{t,r}).$$

Applying the chain rule gives

$$\begin{aligned} \frac{\partial L_t}{\partial \ell_{t,r}} &= - \sum_{v=1}^V \frac{(y_t)_v}{p_{t,v}} \frac{\partial p_{t,v}}{\partial \ell_{t,r}} \\ &= - \sum_{v=1}^V (y_t)_v (\mathbf{1}_{v=r} - p_{t,r}) = p_{t,r} - (y_t)_r. \end{aligned} \quad (21)$$

Thus, in vector form,

$$\frac{\partial L_t}{\partial \ell_t} = p_t - y_t. \quad (22)$$

Since the Jacobian of ℓ_t with respect to h_t is W_{out}^\top , the upstream gradient at the representation interface is

$$u_t \triangleq \frac{\partial L_t}{\partial h_t} = \left(\frac{\partial \ell_t}{\partial h_t} \right)^\top \frac{\partial L_t}{\partial \ell_t} = W_{\text{out}}^\top (p_t - y_t). \quad (23)$$

For a token set \mathcal{T} , the corresponding representation-parameter gradient is

$$\nabla_{\theta_{\text{rep}}} L(\mathcal{T}) = \frac{1}{|\mathcal{T}|} \sum_{t \in \mathcal{T}} J_t^\top u_t. \quad (24)$$

Thus, $\{u_t\}$ are the common upstream optimization signals that drive updates of the representation-producing parameters through the Jacobian mapping.

Consider two token sets \mathcal{T}_1 and \mathcal{T}_2 . Their representation-parameter gradient inner product is

$$\begin{aligned} \langle \nabla_{\theta_{\text{rep}}} L(\mathcal{T}_1), \nabla_{\theta_{\text{rep}}} L(\mathcal{T}_2) \rangle &= \left\langle \frac{1}{|\mathcal{T}_1|} \sum_{t \in \mathcal{T}_1} J_t^\top u_t, \frac{1}{|\mathcal{T}_2|} \sum_{t' \in \mathcal{T}_2} J_{t'}^\top u_{t'} \right\rangle \\ &= \frac{1}{|\mathcal{T}_1| |\mathcal{T}_2|} \sum_{t \in \mathcal{T}_1} \sum_{t' \in \mathcal{T}_2} u_t^\top (J_t J_{t'}^\top) u_{t'}. \end{aligned} \quad (25)$$

Accordingly, their exact representation-parameter cosine alignment is

$$\cos(\nabla_{\theta_{\text{rep}}} L(\mathcal{T}_1), \nabla_{\theta_{\text{rep}}} L(\mathcal{T}_2)) = \frac{\sum_{t \in \mathcal{T}_1} \sum_{t' \in \mathcal{T}_2} u_t^\top (J_t J_{t'}^\top) u_{t'}}{\left\| \sum_{t \in \mathcal{T}_1} J_t^\top u_t \right\| \left\| \sum_{t' \in \mathcal{T}_2} J_{t'}^\top u_{t'} \right\|}, \quad (26)$$

where the segment-length normalization factors cancel in the cosine.

Eq. 26 shows that exact alignment depends on both upstream gradients and Jacobian-induced interactions. Exact step-level evaluation of these interactions would require isolating each step loss and explicitly backpropagating it through θ_{rep} , leading to repeated per-step gradient computation. We therefore use an interface-level surrogate that preserves the upstream optimization signals while avoiding explicit construction of the Jacobian-induced geometry, in line with scalable data valuation methods that approximate gradient information in proxy spaces. This yields the representation-level proxy

$$g(\mathcal{T}) \triangleq \frac{1}{|\mathcal{T}|} \sum_{t \in \mathcal{T}} u_t. \quad (27)$$

For the k -th reasoning step and the answer segment, we define

$$g_k \triangleq g(\mathcal{T}_k), \quad g_{\text{ans}} \triangleq g(\mathcal{T}_{\text{ans}}).$$

Using this proxy, the gradient-space quantities in Sec. 2.2 are instantiated as

$$\widehat{\text{Score}}_k = \begin{cases} \widehat{A}_k^{\text{ans}}, & k = 1, \\ \alpha \widehat{A}_k^{\text{ans}} + (1 - \alpha) \widehat{A}_k^{\text{hist}}, & k > 1, \end{cases} \quad (28)$$

Algorithm 1 GRACE reasoning data curation

Require: Reasoning dataset \mathcal{D} , initial model f_{θ_0} , warm-up ratio γ , selection ratio ρ , balance coefficient α

Ensure: Curated subset \mathcal{S}

- 1: Warm up f_{θ_0} on a subset of \mathcal{D} with ratio γ to obtain f_{θ} .
 - 2: Keep f_{θ} fixed during scoring and let W_{out} be its output projection.
 - 3: **for** each sample $z_i = (x_i, \mathbf{s}_i, a_i) \in \mathcal{D}$ **do**
 - 4: Run a forward pass with model f_{θ} to obtain token probabilities p_t .
 - 5: Compute upstream signals: $u_t \leftarrow W_{\text{out}}(p_t - y_t)$, where y_t is the ground-truth token.
 - 6: **for** each reasoning step $s_{i,k}$ **do**
 - 7: $g_{i,k} \leftarrow |\mathcal{T}_{i,k}|^{-1} \sum_{t \in \mathcal{T}_{i,k}} u_t$.
 - 8: **end for**
 - 9: $g_{i,\text{ans}} \leftarrow |\mathcal{T}_{i,\text{ans}}|^{-1} \sum_{t \in \mathcal{T}_{i,\text{ans}}} u_t$.
 - 10: **for** each reasoning step $s_{i,k}$ **do**
 - 11: **if** $k = 1$ **then**
 - 12: $\widehat{\text{Score}}_{i,1} \leftarrow \cos(g_{i,1}, g_{i,\text{ans}})$.
 - 13: **else**
 - 14: $\widehat{r}_{i,k} \leftarrow \text{Normalize} \left(\sum_{j < k} \omega_{k,j} g_{i,j} \right)$.
 - 15: $\widehat{\text{Score}}_{i,k} \leftarrow \alpha \cos(g_{i,k}, g_{i,\text{ans}}) + (1 - \alpha) \cos(g_{i,k}, \widehat{r}_{i,k})$.
 - 16: **end if**
 - 17: **end for**
 - 18: $V(z_i) \leftarrow K_i^{-1} \sum_{k=1}^{K_i} \widehat{\text{Score}}_{i,k}$.
 - 19: **end for**
 - 20: Select \mathcal{S} as the top $\lceil \rho |\mathcal{D}| \rceil$ samples ranked by $V(z_i)$.
 - 21: **return** \mathcal{S}
-

where

$$\widehat{A}_k^{\text{ans}} \triangleq \cos(g_k, g_{\text{ans}}), \quad \widehat{A}_k^{\text{hist}} \triangleq \cos(g_k, \widehat{r}_k), \quad \widehat{r}_k \triangleq \text{Normalize} \left(\sum_{j < k} \omega_{k,j} g_j \right).$$

Thus, $\widehat{\text{Score}}_k$ is the computable representation-level approximation of the gradient-space utility Score_k . The coefficients $\omega_{k,j}$ can instantiate several common history aggregation strategies:

$$\omega_{k,j} = \begin{cases} 1 & \text{Uniform,} \\ \frac{1}{k-1}, & \\ \frac{\mathbf{1}\{\max(1, k-W) \leq j < k\}}{\min(W, k-1)}, & \text{Sliding window,} \\ \frac{\beta^{k-1-j}}{\sum_{r=1}^{k-1} \beta^{k-1-r}}, & \text{EMA.} \end{cases}$$

where $W \in \mathbb{N}$ denotes the window size, $\beta \in [0, 1)$ is the decay factor, and $\mathbf{1}\{\cdot\}$ is the indicator function.

D Detailed Algorithm

Algorithm 1 provides the complete curation procedure of GRACE, including model warm-up, forward-only proxy extraction, step-level scoring, sample-level aggregation, and top- ρ subset selection.

E Experimental Details

Training data. We post-train on MMathCoT-1M [3], a large-scale multimodal mathematical reasoning corpus with chain-of-thought supervision. Since GRACE evaluates step-level optimization signals, we use reasoning traces with at least eight reasoning steps as the default candidate pool,

which provides sufficient granularity for stable step-level utility estimation. Preliminary experiments show that training on the full MMathCoT-1M does not improve downstream performance over this reasoning-rich pool, suggesting that this filtering does not compromise training effectiveness. Unless explicitly stated otherwise, all reported full-data baselines and selection ratios are defined with respect to this ≥ 8 -step candidate pool.

Backbone models. Our default backbone is Qwen3-VL-2B-Instruct [11]. To examine the transferability of GRACE-selected subsets, we additionally post-train Qwen2.5-VL-3B [25], LLaVA-1.5-7B [26], and Qwen3-VL-8B-Instruct on the same curated subset, without re-running data selection.

For data scoring, we warm up the initial model on a $\gamma = 0.05$ subset of the candidate pool to obtain the fixed scoring model f_θ , and use a single warm-up checkpoint by default. The warm-up subset is used only to obtain the fixed scoring model and is not counted as post-training data. For fairness, all gradient- and proxy-based baselines use the same warm-up checkpoint when applicable. The default selection ratio is $\rho = 0.2$. The historical reference direction \hat{r}_k uses uniform aggregation ($\omega_{k,j} = 1/(k-1)$, i.e., the historical average), and the balance coefficient is fixed to $\alpha = 0.7$. Post-training and evaluation are conducted with the ms-swift framework [38].

Baselines. We compare GRACE against two families of baselines: (i) *heuristic selectors*—Random (uniform sampling), Longest (longest reasoning traces by token length), and Stepmax (traces with the largest number of steps); (ii) *state-of-the-art data curation methods*—LESS [12], a gradient-projection-based influence method; ICONS [7], a cross-task influence-consensus selector; and CADC [13], a recent curriculum-aware data curator. For fair comparison, all baselines select subsets at the same ratio ρ from the same candidate pool and are post-trained with identical training recipes.

Benchmarks. We evaluate the post-trained models on a diverse suite of multimodal benchmarks using the VLMEvalKit [39] backend integrated in ms-swift, covering three categories:

- *general visual question answering and perception*—HallusionBench [18], ScienceQA [19], MMBench [20], MME (Perception and Cognition) [21];
- *multi-task and multi-image reasoning*—MMT-Bench (single-image) and MMT-Bench_MI (multi-image) [22];
- *mathematical reasoning*—MathVista [23], MathVision_MINI, and MathVision (full) [24].

We report task-specific metrics for each benchmark, and additionally report relative average performance (*Rel. Avg.*) normalized by the full-data training baseline. For compactness, tables abbreviate HallusionBench as Hallusion, ScienceQA as SQA, MME Perception/Cognition as Perc./Cog., and MMT-Bench single-/multi-image settings as SI/MI.

Given B evaluation entries, including benchmark sub-scores reported separately, we compute the relative score of a selected subset \mathcal{S} on entry b as

$$R_b(\mathcal{S}) = \frac{m_b(\mathcal{S})}{m_b(\mathcal{D}_{\text{full}})} \times 100,$$

where $m_b(\cdot)$ denotes the metric of entry b , and $\mathcal{D}_{\text{full}}$ denotes the full ≥ 8 -step candidate pool. The relative average is then

$$\text{Rel. Avg.} = \frac{1}{B} \sum_{b=1}^B R_b(\mathcal{S}).$$

Implementation framework. All post-training experiments are implemented with ms-swift v3.12.1, following the official recommended SFT recipe for vision-language models. We use PyTorch 2.9.0 with CUDA 12.8 and cuDNN 9.10.2, and use DeepSpeed v0.17.6 with ZeRO-2 optimization for distributed training.

Post-training configuration. Unless otherwise specified, all models are fine-tuned for one epoch with LoRA. We use bfloat16 precision, FlashAttention, padding-free training, sequence packing, and gradient checkpointing. LoRA is applied to all linear layers with rank 8 and scaling factor 32, while the vision encoder and multimodal aligner are frozen. The learning rate is set to 1×10^{-4} with a

Table 6: Full hyperparameter results for candidate pool and warm-up strategy on Qwen3-VL-2B at $\rho = 0.2$. For four-checkpoint scoring, 0.25–1.0 denotes checkpoints at 25%, 50%, 75%, and 100% warm-up progress.

Variant	γ	Hist.	α	Hallusion	SQA	MMBench	MME		MMT		MathVista	MathVision		Rel. Avg.
							Perc.	Cog.	SI	MI		MINI	Full	
≥ 8 -step pool	–	–	–	43.7	80.2	69.3	1517.3	656.1	55.0	53.4	52.5	14.7	16.4	100.0
Full w/o step filter	–	–	–	43.2	83.4	73.5	1526.0	593.6	56.0	54.6	50.1	14.9	15.1	99.3
Warm-up 25%	0.25	uniform	0.5	46.2	83.5	72.5	1506.7	622.9	56.7	54.4	50.3	15.0	13.8	99.6
Four checkpoints	0.25–1.0	uniform	0.5	45.6	85.2	72.4	1508.5	650.0	57.2	56.2	50.7	14.8	15.8	101.7
No warm-up	0	uniform	0.5	12.5	72.2	70.4	1486.7	465.7	54.6	53.1	51.4	15.8	16.8	89.6

Table 7: Full hyperparameter results for history aggregation on Qwen3-VL-2B at $\rho = 0.2$. All variants use $\gamma = 0.05$ and $\alpha = 0.5$. **Bold** and underlined values denote the best and second-best *Rel. Avg.*, respectively.

Hist.	Param.	γ	α	Hallusion	SQA	MMBench	MME		MMT		MathVista	MathVision		Rel. Avg.
							Perc.	Cog.	SI	MI		MINI	Full	
Window	$W = 2$	0.05	0.5	46.1	83.0	72.7	1508.8	665.0	59.3	57.0	52.9	14.5	17.2	103.5
	$W = 3$	0.05	0.5	45.8	84.6	72.8	1504.5	692.1	57.2	55.8	52.0	17.1	16.7	104.6
	$W = 4$	0.05	0.5	44.5	83.7	73.3	1504.0	610.4	57.0	54.9	54.7	17.8	16.5	103.6
	$W = 5$	0.05	0.5	44.3	85.8	74.4	1494.6	577.5	57.7	56.5	53.3	16.4	16.8	103.0
	$W = 6$	0.05	0.5	45.1	82.8	71.4	1501.8	693.9	57.3	55.3	44.2	17.4	15.8	102.0
	$W = 8$	0.05	0.5	47.5	84.9	73.3	1486.8	652.9	57.5	55.0	53.8	17.1	16.1	104.2
EMA	$\beta = 0.70$	0.05	0.5	46.4	84.1	73.3	1505.0	671.8	56.7	55.9	51.1	18.4	16.3	104.7
	$\beta = 0.75$	0.05	0.5	45.6	84.7	73.5	1506.2	658.6	57.3	55.8	49.8	19.4	16.1	104.7
	$\beta = 0.80$	0.05	0.5	46.6	84.3	72.7	1496.4	669.6	57.7	55.5	51.0	20.1	16.4	<u>105.7</u>
	$\beta = 0.85$	0.05	0.5	46.0	85.5	74.3	1493.9	588.9	57.2	55.8	52.9	18.8	16.1	104.1
	$\beta = 0.90$	0.05	0.5	46.1	83.8	72.7	1508.2	666.1	57.1	54.5	54.1	17.1	16.4	104.1
	$\beta = 0.95$	0.05	0.5	45.9	84.5	72.4	1498.1	651.1	57.1	56.0	53.8	17.4	15.3	103.4
	$\beta = 0.99$	0.05	0.5	45.9	85.5	73.1	1483.4	610.7	57.3	55.8	51.7	15.8	15.5	101.7
Uniform	–	0.05	0.5	47.3	85.5	75.1	1509.6	678.2	57.5	56.1	52.2	19.4	16.5	106.6

warm-up ratio of 0.05. The per-device batch size is 1, the gradient accumulation step is 2, and the maximum sequence length is 4096. Optimizer and scheduler settings follow the default ms-swift SFT configuration unless otherwise stated.

Hardware. Experiments are conducted on a server with eight NVIDIA A800-SXM4-80GB GPUs and approximately 1.0 TiB system memory, running Ubuntu 22.04.5 LTS.

F Full Hyperparameter Results

We provide the full per-benchmark hyperparameter results in Tables 6–8.

Table 8: Full hyperparameter results for the balance coefficient α on Qwen3-VL-2B at $\rho = 0.2$. All variants use $\gamma = 0.05$. **Bold** and underlined values denote the best and second-best *Rel. Avg.*, respectively.

Hist.	Param.	α	Hallusion	SQA	MMBench	MME		MMT		MathVista	MathVision		Rel. Avg.
						Perc.	Cog.	SI	MI		MINI	Full	
Uniform –		0.9	46.6	84.7	72.4	1506.0	683.9	56.3	54.2	52.9	21.4	17.9	<u>107.7</u>
		0.8	46.2	82.5	71.5	1496.1	678.2	56.3	54.0	53.4	18.4	17.1	104.7
		0.7	46.8	85.0	73.8	1512.3	682.9	58.5	56.3	54.2	21.7	17.2	108.8
		0.6	45.7	83.5	71.1	1501.3	682.1	56.9	54.1	52.7	16.4	16.5	103.2
		0.5	47.3	85.5	75.1	1509.6	678.2	57.5	56.1	52.2	19.4	16.5	106.6
		0.4	44.0	81.6	70.0	1494.5	686.1	54.7	53.2	52.5	17.1	15.7	101.7
		0.3	47.1	82.7	70.0	1496.6	667.9	55.2	53.8	51.1	18.4	16.5	103.6
		0.2	45.7	85.1	70.8	1500.8	665.0	56.9	54.8	50.3	17.1	16.0	102.8
		0.1	43.9	83.8	71.4	1516.0	647.5	56.6	55.1	53.6	13.8	15.9	100.8
Window $W = 3$		0.9	46.3	83.7	71.5	1493.9	686.4	57.0	54.7	54.6	21.7	16.6	107.2
		0.8	45.1	81.9	71.8	1510.2	677.5	57.2	54.7	52.5	18.4	17.0	104.6
		0.7	44.5	84.0	72.5	1496.6	673.6	56.8	54.3	52.3	17.8	16.4	103.7
		0.6	44.7	82.6	71.1	1503.7	695.0	56.3	54.2	52.1	15.5	16.2	102.0
		0.5	45.8	84.6	72.8	1504.5	692.1	57.2	55.8	52.0	17.1	16.7	104.6
		0.4	46.1	83.7	71.1	1496.1	690.0	57.1	54.7	53.1	17.4	15.6	103.6
		0.3	46.4	83.7	71.8	1505.3	670.0	56.4	53.9	53.0	18.8	15.5	104.0
		0.2	44.1	83.1	72.0	1513.2	677.1	56.1	53.7	52.9	17.8	15.5	102.8
		0.1	45.6	83.6	71.6	1503.0	651.8	56.0	55.2	51.7	18.4	14.7	102.6
EMA $\beta = 0.8$		0.9	46.1	83.6	72.5	1491.7	661.8	57.2	54.7	53.5	17.4	17.0	104.4
		0.8	45.2	82.9	70.2	1498.7	672.5	56.7	54.5	51.7	16.4	17.2	103.0
		0.7	44.1	83.7	71.7	1511.6	689.3	56.2	54.7	52.4	15.8	16.7	102.8
		0.6	47.4	83.9	70.5	1501.0	692.9	55.3	53.7	53.6	18.1	17.4	105.1
		0.5	46.6	84.3	72.7	1496.4	669.6	57.7	55.5	51.0	20.1	16.4	105.7
		0.4	45.5	82.7	71.6	1498.3	677.9	56.4	54.6	53.1	17.4	16.9	104.0
		0.3	45.0	84.5	71.4	1506.5	659.6	55.8	53.9	52.5	17.4	16.8	103.4
		0.2	44.9	85.1	72.3	1512.8	635.4	56.4	54.5	54.2	16.1	16.3	102.7
		0.1	43.9	82.4	69.7	1502.4	656.1	55.9	53.7	53.6	16.4	16.7	102.1